Volume 9
Number 30
14 August 2021
Pages 5917–6094

Journal of Materials Chemistry B

Materials for biology and medicine

rsc.li/materials-b

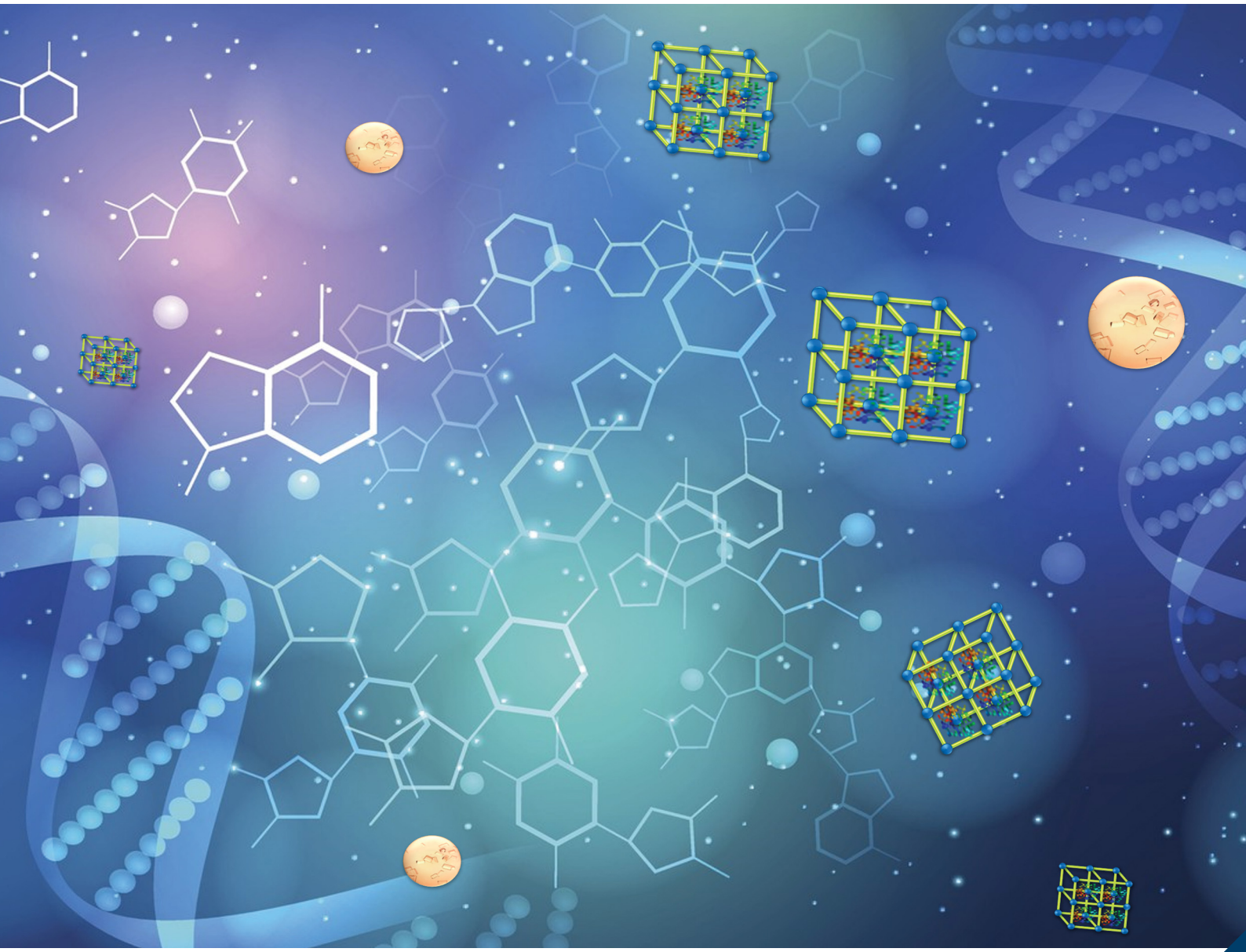

ISSN 2050-750X

ROYAL SOCIETY OF CHEMISTRY

REVIEW ARTICLE

Niveen M. Khashab *et al.*

Biocompatibility and biodegradability of metal organic frameworks for biomedical applications

Indexed in Medline!

Journal of Materials Chemistry B

ROYAL SOCIETY OF CHEMISTRY

REVIEW

View Article Online
View Journal | View Issue

Cite this: *J. Mater. Chem. B*, 2021, **9**, 5925

Biocompatibility and biodegradability of metal organic frameworks for biomedical applications

Namita Singh, Somayah Qutub and Niveen M. Khashab *

Metal organic frameworks (MOFs) are a unique class of smart hybrid materials that have recently attracted significant interest for catalysis, separation and biomedical applications. Different strategies have been developed to overcome the limitations of MOFs for bio-applications in order to produce a system with high biocompatibility and biodegradability. In this review, we outline the chemical and physical factors that dictate the biocompatibility and biodegradability characteristics of MOFs including the nature of the metal ions and organic ligands, size, surface properties and colloidal stability. This review includes the *in vitro* biodegradation and *in vivo* biodistribution studies of MOFs to better understand their pharmacokinetics, organ toxicity and immune response. Such studies can guide the design of future bio-friendly systems that bring us closer to safely translating these platforms into the pharmaceutical consumer market.

Received 9th May 2021,
Accepted 18th June 2021

DOI: 10.1039/d1tb01044a

rsc.li/materials-b

1. Introduction

Metal organic frameworks (MOFs) are composed of multiple metal ions or metal clusters and organic bridging ligands and are considered as the prime members of inorganic–organic hybrid materials.[1] MOFs are widely studied for their tunable topologies and functionalities. However, the main incentive leading to the investigation of MOFs is their tailorable composition and high and uniform porosity which make them preferable for various useful applications such as catalysis,[2] gas storage and separation.[3–5] The modulation of the MOF size into a nano-MOF (nMOF) and the organic/inorganic nature have opened the door for unlimited biological applications. Moreover, the functionalization of the organic linker or strut during or after synthesis drastically enhances the physiological properties of these nMOFs.[6–12] For instance, it can decrease cytotoxicity, improve colloidal stability and promote suitable degradation rates and efficient cellular uptake. Compared to the conventional nanocarriers (like inorganic zeolites and silica nanomaterials and organic nanocarriers such as lipids and polymers), the nMOFs possess the right properties that make them promising candidates for biological applications. First, nMOFs can be synthesized using biocompatible components with a tolerable pharmacokinetic profile. Second, large surface area and small pore volume can guarantee a high loading capacity and great biopreservation properties for the optimal drug delivery system. Wolfgang and co-worker also studied in detail the benefits of using MOFs for drug delivery in comparison to mesoporous silica and dendrimers.[13] Similarly, the Falcaro group compared the protective properties of ZIFs to the inorganic nanoparticles, $CaCO_3$ and mesoporous silica.[14] They encapsulated the HRP enzyme into the three systems and monitored the activity of the encapsulated enzyme after exposing them to harsh conditions. ZIF-8 showed superior protective properties and retained most of the enzyme activity. Also, it showed a controlled release of the cargo under slightly acidic conditions, which makes MOFs ideal for drug delivery. Moreover, MOFs need to be stable enough to deliver the molecule of interest to the targeted tissue but also be degraded and readily eliminated from the body without endogenous accumulation. The presence of labile metal ligand bonds endows nMOFs with rapid degradation to release the loaded material. Therefore, nMOFs are widely investigated as a delivery vehicle for imaging, diagnosis, treatment of diseases and biosensing (Scheme 1).[15–27]

Many reviews have been published on bio-MOFs or biomimetic MOFs, which included the various applications of these platforms in nanomedicine.[28–34] In this review, we focus on the different factors that affect or determine the biocompatibility and biodegradability of MOFs. Biocompatibility depends on the nature of the coordination metal and the organic linker in addition to the overall physical properties including size, shape and surface charge. As for biodegradability, we reviewed the available *in vivo* and *in vitro* data to conclude the best profiles that have been reported so far. Moreover, we discuss the future directions of these intriguing classes of smart materials to speed their translation into actual pharmaceutical and biomedical applications.

Smart Hybrid Materials (SHMs) Laboratory, Advanced Membranes and Porous Materials Center, King Abdullah University of Science and Technology (KAUST), Thuwal 23955-6900, Kingdom of Saudi Arabia.
E-mail: niveen.khashab@kaust.edu.sa

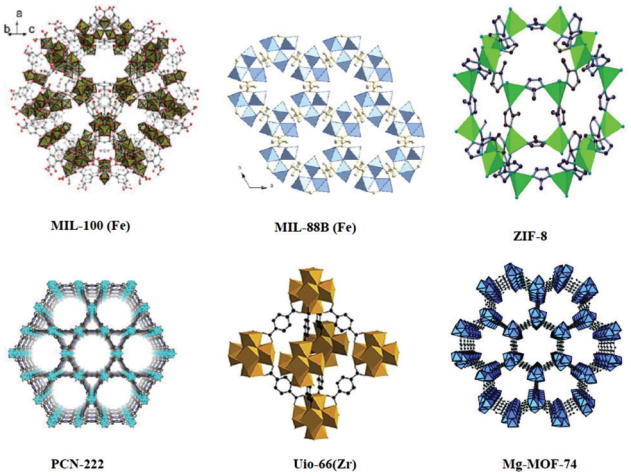

Scheme 1 Structures of MOFs. [MIL-100(Fe).[105] Reproduced with permission from ref. 105. Copyright 2016 RSC. MIL-88B(Fe).[106] Reproduced with permission from ref. 106. Copyright 2013 American Chemical Society. ZIF-8.[107] Reproduced with permission from ref. 107. Copyright 2018 MDPI. PCN-222.[108] Reproduced with permission from ref. 108. Copyright 2019 American Chemical Society. Uio-66(Zr).[109] Reproduced with permission from ref. 109. Copyright 2019 Elsevier Mg-MOF-74.[110] Reproduced with permission from ref. 110. Copyright 2016 Wiley]

2. Biocompatibility of MOFs

2.1. Nature of the building blocks

The biocompatibility of MOF precursors is very essential for the overall system to fall within the bioavailability range. The toxicity of metals and the ligands has been assessed compared to that of the assembled MOFs where a direct correlation can be deduced.[35,36] The toxicity of MOFs depends on several other factors such as the kinetics of degradation, bio-distribution, accumulation in tissues and organs, excretion from the body, applications and balance between risks and benefits and so on.[28,37–44] The MOFs that are used for biomedical applications usually consist of metals that are essential for the body such as iron, zinc and magnesium.

2.1.1. Metal ions. The most compatible cations for the preparation of biocompatible MOFs are simply selected based on a lethal dose and a daily dose of metals. The lethal dose is considered as the median lethal dose (LD50), the amount of the compound that kills half the members of a given population after a specific duration. The experimental results of the oral lethal dose to rats reveal that Ca, Mg, Zn, Fe, Ti, and Zr are appropriate metals for the construction of biocompatible MOFs.[28] However, these doses vary with chemical formulation (counter anion and oxidation state). Another concern is the daily dose, as a few metals are required by humans in mg per day amounts and recognized as essential trace elements.[45] Metals such as Zr and Ti are poorly absorbed by the body and not considered as toxic for specific applications, such as their use in cosmetics ($LD_{50} > 25$ g kg^{-1}).

2.1.2. Ligands. A wide range of organic ligands are available for the construction of biocompatible MOFs and can be classified into exogenous and endogenous ligands. The exogenous ligands are synthetic linkers that are not naturally found in the body. Therefore, it is necessary for them to be excreted or metabolized after the *in vivo* application. This category includes polycarboxylates, phosphonates, sulfonates, imidazolates, amines, pyridyl and phenolates. Recent biocompatibility data revealed that a few polycarboxylates (terephthalic, trimesic, 2,6-naphthalenedicarboxylic acids) and imidazolate linkers are not very toxic due to their high polarity and ease of removal under physiological conditions (Scheme 2).[28] The functionalization of exogenous linkers with apolar and polar functional groups such as amino, nitro, chloro, bromo, carboxylate, methyl, perfluoro, *etc.* can tune their ADME (absorption, distribution, metabolism, and excretion) behaviors.[6,7,46] The presence of functional groups not only modulates the host–guest interactions but also influences the flexibility of the framework for better absorption and delivery of the cargo biomolecules.[7,46] There are various examples of functionalized MOFs such as MIL-53(Fe),[47] MIL-88B(Fe),[48] UiO-66(Zr),[49] and MIL-125(Ti)[50] decorated with polycarboxylate linkers. In addition, organically modified porous Zn imidazolate solids can also be included in this series.[51–55]

On the other hand, ligands or linkers that are naturally found in the body such as amino acids, peptides, proteins, nucleobases, carbohydrates and porphyrins are referred to as endogenous linkers. For bio-applications, the use of endogenous molecules in MOFs can reduce the risk of adverse effects as they can be absorbed safely by the body. A notable number of MOFs containing the endogenous linkers has been reported so far.[56] The endogenous molecules that have been used as linkers for the preparation of MOFs are aspartate,[57] adenine,[58] fumarate,[59] muconate[60] and cyclodextrin[61] (Scheme 2). However, only a few of them have been utilized for bio-applications due to the stability and porosity limitations.[62]

2.2. Physiological properties

2.2.1. Size. The size of nMOFs is an important factor that impacts the biodistribution, circulatory lifetime *in vivo* and targeting abilities. Studies in this direction suggest that the optimal size would be <200 nm.[63–66] Controlling the size of the nMOFs has attracted much attention and included various methods such as hydrothermal,[67] hydro/solvothermal,[68] reverse-phase microemulsion,[69] sonochemical,[70] and microwave-assisted synthesis[71] in addition to the conventional techniques of using

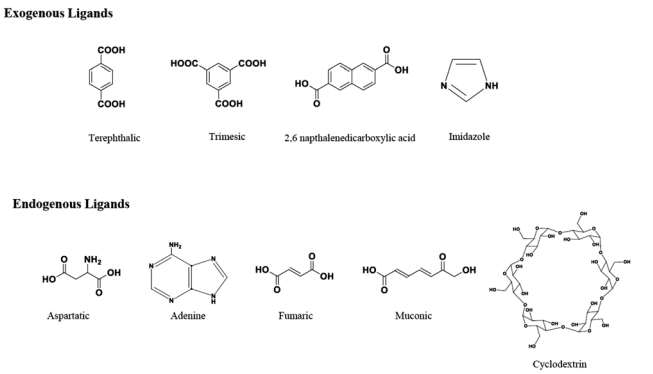

Scheme 2 Presentation of the exogenous and endogenous ligands.

growth inhibitors for delaying the nucleation process,[68] the nanotemplate for confining the space[72] and tuning the ratio of surfactants.[73] However, the exact relationship between the size of the nMOFs and their impact on the body is still uncertain.[74] A size study of the Zr-nMOFs ranging between 30 and 190 nm was conducted by Zhou and co-workers on cellular uptake by HeLa cells.[63] This result revealed that the cellular uptake of the MOF PCN-224 was size dependent in the order of 90 nm > 60 nm > 30 nm > 140 nm > 190 nm. Liu and co-workers studied the size effect of drug-loaded MOFs (DOX@AZIF-8) on the *in vivo* biodistribution, cellular uptake and killing effect on tumor cells. They found that the 60 nm size of DOX@AZIF-8 showed a prolonged blood circulation and higher tumor uptake compared to the larger size of DOX@AZIF-8 (Fig. 1).[65] Zhu's group conducted detailed research to investigate and compare the biosafety of the micron- and nanoscale Mg-MOF74 (m/n-Mg-MOF74) particles.[66] The study revealed that both micron/nanoscale Mg-MOF74 showed good biocompatibility and n-Mg-MOF74 showed a wider range of safe concentrations compared to the micron-sized particles. Furthermore, a suitable dose of n-Mg-MOF74 achieved early osteogenic promotion and angiogenic stimulation effects, suggesting nanoscale Mg-MOF74 as a better option over the micron-sized particles. It could be concluded that a size of up to 200 nm has unique physiological properties.[64] The size of the particles determines their velocity and diffusion in the body as well as influences their response whether to be internalized in tumor cells or cleared from the body by macrophages or the renal system to protect the body from their side effects.[75]

2.2.2. Stability. The nMOFs are constructed with different kinds of metal ions and organic linkers and their structural stability is a potential concern for bio-applications. The structural stability of MOFs in aqueous media is influenced by many factors such as metal–ligand bond strength, the basicity of the ligand, coordination number and the oxidation state of the metal center and framework dimensionality.[76] The stability of MOFs can also be improved by introducing catenation or interpenetration into the framework and employing a linker of higher pK_a value.[77] For bio-applications, a certain extent of chemical stability is required for approaching the target sites and upon changing the pH and composition of the body fluids, degradability of the framework becomes necessary to release the cargo. MOF-5 and MOF-177, which are composed of zinc and poly-carboxylates ions, do not show stability in water and decompose rapidly.[78,79] MOF-5 was observed to be very moisture sensitive due to its relatively weak metal–oxygen coordination bonds. On the other hand, some MOFs were reported to show stability under hydrothermal and humid conditions. MOFs based on Al-carboxylate, such as Al-MIL-53, were stable in 50% humidity for 30 days.[80] Ni-CPO-27 MOFs were stable in bovine serum at 37 °C for 4 days.[81] MOF PCN-222 showed exceptional hydrothermal stability owing to the assembled Zr_6 cluster, which is considered as one of the most stable secondary building units (SBUs).[82] Gassensmith's group studied the stability of ZIF-8 in common laboratory buffers, cell media, and serum and showed surface chemistry changes affecting the interpretation of cellular uptake and cargo release (Fig. 2).[83] Other MOFs, such as MIL-100(Fe)[84] and UiO-66(Zr)[82], were stable in water. However, UiO-66(Zr) and MIL-100(Fe) degraded within a few hours after being dispersed in phosphate buffer.[85] The complete degradation of MIL-88A(Fe) occurred in phosphate buffer after several days.[86] The MOF stability in body fluid cannot be predicted by their stability in water and further studies are needed in full culture media or simulated body fluids for a better understanding of the degradation mechanism.

2.2.3. Surface. To achieve the bio-adhesive and targeting properties, an appropriate design of the nMOF system becomes necessary. Along with the size and stability, the other

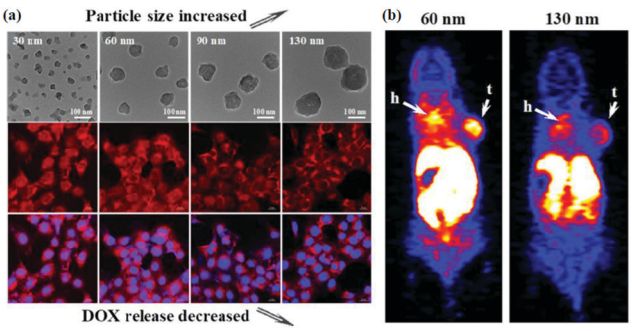

Fig. 1 (a) DOX@AZIF-8 showed size-dependent cellular uptake and drug release. (b) 60 nm ^{64}Cu-DOX@AZIF-8 and 130 nm ^{64}Cu-DOX@AZIF-8 exhibited a significant difference in the tumor accumulation. Reproduced with permission from ref. 65. Copyright 2018 American Chemical Society.

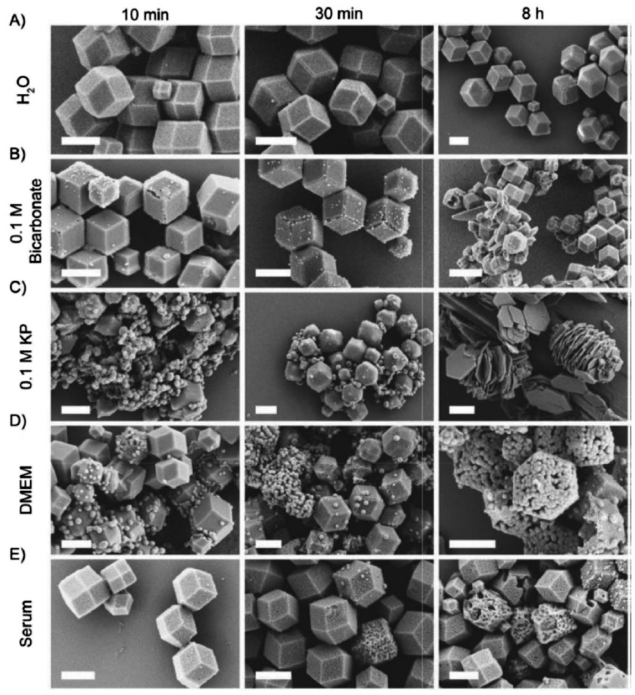

Fig. 2 SEM images of ZIF-8 incubated in (A) water (pH 7.8), (B) 0.1 M bicarbonate buffer (pH 9.5), (C) 0.1 M KP buffer (pH 7.4), (D) DMEM (pH 7.6), and (E) serum (bovine serum, pH 7.9). (scale bar: 1 μm.) Reproduced with permission from ref. 83. Copyright 2019 Taylor & Francis.

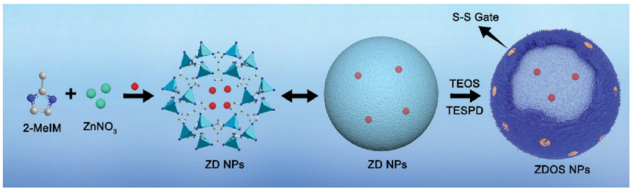

Fig. 3 Preparation of the ZIF-8@DOX@organosilica (ZDOS) NPs. Reproduced with permission from ref. 12. Copyright 2019 American Chemical Society.

biophysical properties of nMOFs such as surface hydrophilicity and the nature and density of the ligands at their surface are also important as they regulate the interaction of nMOFs with physiological medium components like proteins, lipids, ions, *etc.* The outer surface of nMOFs can be modified to tune the stability and the ability of nMOFs to circulate in the bloodstream until the successful targeted delivery. The most common way discovered to modify the surface properties of nMOFs is post-synthetic modification, which includes the coating of a functional layer on the surface. As the functional coating material, organic polymers, silica shells and lipid bilayers have been used and reported as nMOF surface modifiers. Silica, as a coating material for nMOFs, increases the biocompatibility by improving water dispersibility and reducing the decomposition of nMOFs. H.-L. Zhu reported a dual-responsive ZIF-8 nanoscale drug delivery system by functionalizing the organosilica shell with redox-responsive disulfide bridges in its framework.[12] As a disulfide bond is relatively stable in plasma and breaks down in the presence of a high concentration of glutathione (GSH), a controlled degradation is also established (Fig. 3). The nanocarriers maintain their stability under physiological conditions and after internalization into cancer cells, the disulfide linkages are cleaved by the endogenous GSH triggering the release of the encapsulated anti-tumor drug (DOX). Moreover, cell internalization, drug release, cytotoxicity, subcellular localization, and antitumor activity *in vivo* experiments show that ZDOS NPs exhibited negligible hemolytic potential and significantly enhanced anticancer efficiencies compared to the free DOX (Table 1).

Organic polymers are another representative coating material. Polyethylene glycol (PEG), polyvinylpyrrolidone, polyacrylic acid (PAA) and hyaluronic acid (HA) have been most frequently used as surface modifiers. PEG is amphiphilic in nature and its hydrogen bonding capability enhances the hydrophilicity of nMOFs. Furthermore, the PEGylation of nMOFs elongates the circulation time *in vivo* by preventing aggregation, and decreasing opsonization by blood proteins and uptake by the macrophages of the immune system. Forgan and co-workers modified the surface of UiO-66 nanoparticles with PEG *via* a mild conjugation reaction.[11] The PEGylation of UiO-66 made it more stable, dispersed, and generally more favored for cellular uptake. Zr-MOFs degraded very fast in a phosphate medium and so the PEGylation of UiO-66 improved their stability towards phosphate induced degradation and dispersion in aqueous media. Hyaluronic acid (HA) is a hydrophilic biopolymer that can easily bind to the cancer cells by HA-receptor mediated interaction between CD44 or RHAMM receptors that are overexpressed on the cancer cell surface.[87] HA is considered as an ideal coating material for the surface functionalization of nMOFs due to its ability to overcome the poor bio-distribution, lack of tumor-targeting and serious side effects. Yang and coworkers prepared HA modified nMOFs through supramolecular and coordination interactions of the three building blocks, which showed improved stability in physiological fluids.[88]

Lipid bilayer coating has also been applied to nMOFs, yielding a nanocarrier that can efficiently store dye molecules inside the porous scaffold of the MOF. The lipid bilayer coated MIL-100(Fe) nanoparticles showed an incremental increase in the colloidal stability and efficient uptake by the cancer cells.[89] However, no intracellular release was shown for these nanoparticles. H. Engelke's group used the exosome as the coating material for MIL-88A.[90] Exosomes are extracellular vesicles present in the body fluids and coating with exosomes provides an additional advantage compared to an artificial lipid coating. The exosome coated MOFs can effectively shield the carriers from the immune system for a longer circulation time.

Laser or light-responsive pharmaceutical delivery nanoparticles were later on designed by an emulsion approach using a redox-responsive selenium (Se) substituted polymer as the shell and photosensitive porphyrin zirconium metal–organic

Table 1 Biodegradability, biocompatibility and *in vivo* distribution of different MOFs

MOFs	Biodegradability	Biocompatibility *in vitro*[a]	*In vivo* dose and biodistribution
ZIF-8	Stable in water and degrade at pH 6[38,44] and in PBS at pH 7.4[111]	100 μg mL^{-1} [112]	Safe up to 50 mg kg^{-1} (mouse, injection) Accumulate in tumors and liver[38]
MIL-100	Stable in water and degrade in PBS at pH 7.4[113]	1.1 mg mL^{-1} [112]	Safe up to 220 mg kg^{-1} (rat, injection) Accumulate in liver and spleen[114]
MIL-88B	Stable in water and degrade in PBS at pH 7.4[115]	1.26 mg mL^{-1} [112]	Safe up to 110 mg kg^{-1} (rat, injection) Accumulate in liver, spleen, and lungs[116]
Mg-MOF-74	Degrade in water over time[117]	40 μg mL^{-1} [118]	Reported 2 mg mL^{-1} (mouse, injection)[66] No biodistribution data
PCN-222	Stable in water and degrade at acidic pH[119]	160 μg mL^{-1} (IC_{60})[120]	Reported 5 mg kg^{-1} (mouse, injection) Accumulate in lungs and tumors[119]
Uio-66(Zr)	Stable in water and at acidic pH 2, degrade in PBS at pH 7.4[121,122]	Up to 200 μg mL^{-1} (100% viability)[122]	Reported 5 mg kg^{-1} (mouse, injection) Accumulate in liver, spleen, and tumors[123]
CAU-7	Stable in water and degrade in PBS at pH 7.4	Up to 1.5 mg mL^{-1} (100% viability)[93]	No *in vivo* study

[a] IC_{50} is used for *in vitro* biocompatibility unless otherwise indicated.

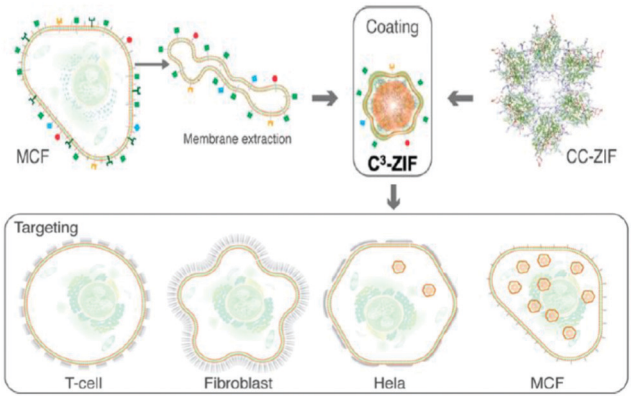

Fig. 4 Preparation of the C^3-ZIF and the cancer cell selectivity of C^3-ZIF. Reproduced with permission from ref. 38. Copyright 2020 American Chemical Society.

frameworks (PCN-224 MOF) as the core.[91] The poly(DH-Se/PEG/PPG urethane)@MOF nanoparticles were loaded with the chemotherapeutic DOX. A combination of chemotherapy and photodynamic therapy, upon irradiation with laser light, causes the cleavage of the poly(DH-Se/PEG/PPG urethane) polymer chain and the release of the encapsulated DOX.

An advanced surface modification based on cancer cell membrane coating technology has been developed by our group to enhance the uptake of nanoparticles, which inherit the antigenic properties of the source cells and can be employed for cancer therapy and vaccination. The zeolitic imidazolate frameworks encapsulating CRISPR/Cas9 (CC-ZIFs) are coated with a cancer cell membrane to enhance the cell-specific gene editing selectivity for tumor cells (Fig. 4).[38]

3. Biodegradability of MOFs

3.1. In vitro

Degradation of MOFs in terms of biosafety needs to be studied before using them as carriers in bio-applications. Generally, degradation studies are carried out in water, phosphate buffer (PBS) and cell culture media at 37 °C at different pH values. However, delivery to the target cells and the impact of carrier degradation are better analyzed *in vitro* using different biological fluids considering the administration route like simulated intestinal fluid (SIF) for the oral route and the simulated body fluid (SBF) for the parenteral route. The degradation of MOFs is influenced by many factors such as metal–ligand strength and environmental conditions as discussed in the Stability section. The pH of the body fluid is the main factor that affects the degradation of MOFs and releases the cargo, which makes MOFs ideal for drug delivery. Our group has reported the release of CRISPR/Cas9 (CC) at pH 5, 6 and 7 using ZIF-8 as the carrier.[92] ZIF-8 showed higher stability at pH 7 and degraded at pH 6 and lower. Also, ZIF-8 showed an enhanced endosomal escape, which was promoted by the protonated imidazole moieties (Fig. 5). Before using MOFs for biomedical applications, it is essential to test the biocompatibility of the building blocks of MOFs as they might have a toxic effect upon the degradation of nMOFs inside the cells. Also, it is important to test the biocompatibility of MOFs with various cell lines as they might show different effects. The *in vitro* biocompatibility of MIL-100 nMOFs based on the three different metal systems (Fe, Al, and Cr) was analyzed.[37] The cytotoxicity test was performed using four epithelial cell lines, lung (A549 and Calu-3) and hepatic (HepG2 and Hep3B), considering pulmonary, ingestion or intravenous exposure modes. The MIL-100 (Fe, Al, Cr) NPs did not induce *in vitro* cell toxicity even after high dosages in A549 and calu-3 (lung) and HepG2 (liver) cell lines. Only the MIL-100(Fe) toxicity was noted in the Hep3B cell line. Hoop *et al.* examined the biocompatibility of ZIF-8 with respect to six different cell lines, representing different body parts (kidneys, skin, breast, blood, bones, and connective tissues).[29] The study revealed that ZIF-8 showed cytotoxicity above a threshold value of 30 μg mL^{-1} due to the effect of the released zinc ions (Zn^{2+}) on the mitochondrial ROS production. As mentioned in the physiological properties section, the size plays an important role in the biocompatibility and degradability of MOFs. The *in vitro* cytotoxicity of micron/nanoscale Mg-MOF74 was evaluated against HeLa cells with a concentration ranging from 50 to 2000 μg mL^{-1}.[66] Both micron and nanoscale Mg-MOF74 showed no significant toxicity to cells below 200 μg mL^{-1}. However, for μ-Mg-MOF74, the cytotoxicity increased above 500 μg mL^{-1} but for n-Mg-MOF74, the cytotoxicity increased above 1000 μg mL^{-1}. The *in vitro* cytotoxicity of CAU-7, a biocompatible bismuth-based MOF, was also measured on HeLa cells in the range of 0–1.5 mg mL^{-1}. The MTS viability values for CAU-7 MOF showed biocompatibility in the range of the used concentrations and no significant difference compared to the untreated cells was observed.[93] The cytotoxicity of IRMOF 1–3 was tested on HepG2 cells with respect to the five concentrations of IRMOFs (5, 10, 15, 20, 25, 30 and 35 mg mL^{-1}).[39] Significant *in vitro* cytotoxicity was not observed for different concentrations of IRMOFs (5, 10, 15, 20, 25, 30 and 35 mg mL^{-1}) and confirmed the biological safety of IRMOFs. Our group studied the *in vitro* uptake of cancer cell membrane coated ZIF-8 with MCF-7, HeLa, HDFn, and aTC cell lines.[38] The cytotoxicity was observed in the concentration range of 50–150 μg mL^{-1} with higher uptake for cancerous cell lines and minimum toxicity for all the cell lines tested. The *in vitro* study is a fast, low cost and effective method for analyzing the behavior of nMOFs and their potential toxicity. However, it does not provide realistic data on the physiological interactions of MOFs in the human body.

3.2. In vivo

In the past few years, more *in vivo* studies have been performed using mice models. Zn, Fe and Zr based MOFs are among the most reported MOFs for biomedical applications. Assessing the biocompatibility of MOFs *in vivo* is very essential as it gives a more defined picture of the toxicity of MOFs in the biological system. For *in vivo* biocompatibility, many parameters need to be considered such as bio-distribution, pharmacokinetics, organ toxicity and immune response. In order to have a robust system with minimum side effects, it is crucial to study these

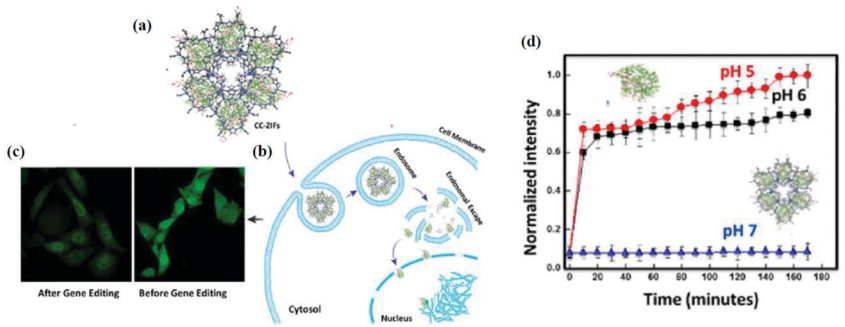

Fig. 5 (a) Cas9/sgRNA within ZIF-8 to form CC-ZIFs. (b) Endosomal escape of CC-ZIFs. (c) CLSM images of cells before and after treatment with CC-ZIFs. (d) The pH dependent release of AF-Cas9/sgRNA from CC-ZIFs. Reproduced with permission from ref. 92. Copyright 2018 American Chemical Society.

parameters. The first parameter is pharmacokinetics, which helps to understand the fate of MOFs once they enter the body until they are excreted (recognition, metabolism, and clearance). Bio-distribution, which is the pattern of MOF accumulation in different organs in the body, is also crucial for the overall assessment of the delivery system. MOFs usually tend to accumulate in the liver[94,95] and kidneys[96] as they are the main organs responsible for NP clearance. Few have reported high accumulations of MOFs in the lungs[97] and spleen.[98] Furthermore, in the case of tumor treatment, MOFs tend to accumulate in tumor tissues due to the high permeability of cancer cells.[99]

Zhu and coworkers investigated the *in vivo* biosafety of Mg-MOF74. The *in vivo* biocompatibility of Mg-MOFs was assessed using the rat model through the intraperitoneal injection administration. The doses were calculated based on the body weight and no significant difference was observed between the treated and untreated rats except for the highest dose, which confirmed the concentration dependency of the *in vivo* toxicity of m/n-Mg-MOF74. The trends of the body weight showed the less impact of n-Mg-MOF74 on the growth compared to their micron-sized particles. The n/m-Mg-MOF74 did not show significant toxicity or damage for the important organs such as the lungs, liver and spleen. Mg-MOF74 showed excellent biosafety and high *in vivo* clearance efficiency with limited myocardial toxicity, which only occurred at very high doses.[66] The *in vivo* toxicity of three different porous iron(III) carboxylate MOF NPs such as MIL-88A, MIL-88B-4CH_3 and MIL-100 was investigated intravenously by evaluating their bio-distribution, metabolism and excretion.[40,41,100] The toxicity of the above mentioned MOFs was assessed by animal behavior, water and food consumption, changes in the body and organ weights, biochemical parameters, oxidative stress, oxidative metabolism, macro and microscopic histological observations, as well as some insights of NP bio-distribution and elimination. During these studies, no death, toxicity or differences in body weight were observed up to 30 days after administration. In the histological examination (lungs, spleen, liver, brain, heart and kidneys), no severe toxicity was observed.

The *in vivo* biocompatibility is also greatly affected by the physiochemical properties of MOFs. Researchers have found innovative methods to make these MOFs more robust with low *in vivo* cytotoxicity. For instance, functionalizing the surface of the MOFs and coating it with more biocompatible materials enhanced the stability and target ability of these systems as mentioned in previous sections. Cell membrane coating is one of the emerging techniques that enable MOFs to exhibit cell-mimicking properties.[101] For example, our group had reported previously the coating of ZIF-8 with cancer membrane, which enhanced the bio-distribution and improved the target ability to cancer cells significantly.[38] The coated ZIF-8 with the MCF-7 membrane had no significant accumulation in the liver and kidneys, whereas it showed a selective, prolonged and 2.5-fold high accumulation in MCF-7 tumor cells compared to the bare ZIF-8 (Fig. 6). Zhuang *et al.* also reported that coating ZIF-8 NPs with RBC had prolonged their circulation in the blood.[96] They encapsulated the uricase enzyme to catalyze uric acid in the plasma.

Further work was performed to enhance the therapeutic efficacy of anticancer therapy by combining different anticancer therapies. For instance, Men *et al.* combined photodynamic therapy with antiangiogenic drugs by wrapping Zr-MOFs with MnO_2.[102] This system was also coated with cancer membrane to enhance the bio-distribution. For the immunological response of MOFs *in vivo*, few reports have emerged in this area as most metal-based MOFs do not trigger the immune system. Therefore, to use MOFs for immunotherapy applications, other immunogenic materials need to be incorporated into the system such as antigens or adjuvants.[43] For example,

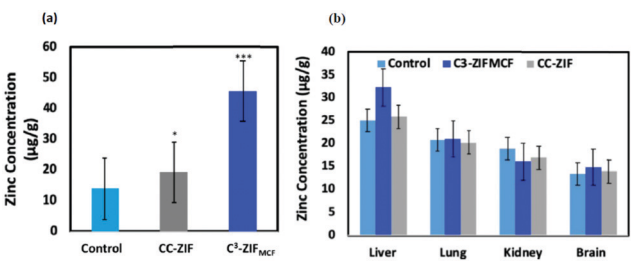

Fig. 6 (a) ICP-MS analysis of Zn in tumors of mice injected with PBS (control), CC-ZIF, or C^3-ZIF_{MCF}. (b) Nanoparticle biodistribution in mice 72 h after injection. Reproduced with permission from ref. 38. Copyright 2020 American Chemical Society.

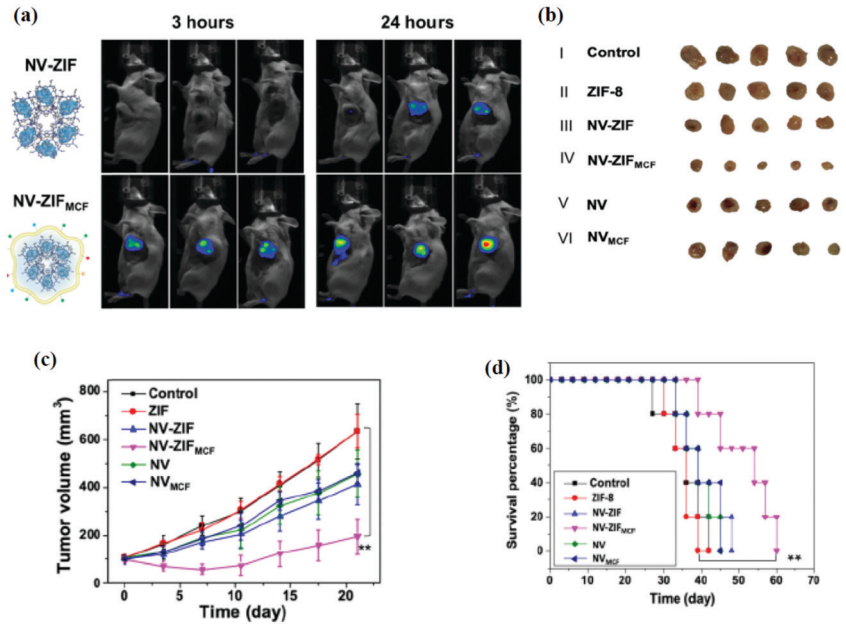

Fig. 7 (a) The *in vivo* fluorescence images of 4T1 cancer-bearing mice after intravenous injection of NV-ZIFs and NV-ZIFMCFs. Images were taken at 3 hours (left) and 24 hours (right) post-injection. (b) Representative images of tumors isolated from mice at the end of various treatments (21 days after injection). (c) Tumor growth curves of different groups of 4T1 cancer-bearing mice after various treatments. (d) Kaplan–Meier survival curve images of 4T1 cancer-bearing mice after various treatments. Reproduced with permission from ref. 44. Copyright 2021 American Association for the Advancement of Science.

aluminum based MOFs and aluminum incorporated MOFs were reported for vaccine-related applications[103] as aluminum is historically used as the adjuvant in vaccines. Moreover, using a tumor antigen had showed promising results as well. Furthermore, our group developed a biocompatible and biodegradable immunotherapeutic delivery system using ZIF-8 for the controlled delivery of nivolumab (NV), a monoclonal antibody checkpoint inhibitor (Fig. 7).[44] The NV-ZIF had shown a higher efficacy than the naked NV to activate T cells in hematological malignancies. We further modified the system by coating the NV-ZIF with the breast cancer cell membrane (MCF-7) to enable the tumor-specific targeted delivery. NV-ZIF$_{MCF}$ showed a greater tumor inhibition in mice and a prolonged retention of NV-ZIF$_{MCF}$ within the tumor microenvironment that resulted in efficient NV delivery. Our system showed superior antitumor effects in hematological and solid tumors in comparison with the free NV. Furthermore, combining immunotherapy with other anticancer therapies can improve the efficacy of the treatment as already reported by many research groups.[42,104]

4. Conclusion

As the interest in MOFs as a smart platform for biomedical applications is constantly increasing, the need to optimize the biocompatibility and biodegradability of these systems is necessary. In this review, we discussed the most significant findings related to the use of MOFs for biomedical applications specifically for drug delivery. We highlighted the critical aspects that promote the best performance including the nature of the building blocks (metal ions and ligands), size, stability and surface chemistry. Moreover, we summarized some of the most recent findings pertaining to the *in vitro* and *in vivo* behavior of nMOF-based systems. It can be easily concluded that all the previously discussed factors significantly affect the pharmacokinetics profile and eventual metabolism and consequently the predicted toxicity of these synthetic biomedical platforms. Although not overwhelmingly critical, metal ions and ligands that are endogenous to the human body are advantageous to a biocompatible design. The platforms with a size of <200 nm with a hydrophilic surface and a relatively stable framework under physiological pH showed the best performance in terms of biocompatibility and bioavailability so far. Although considerable research is currently being conducted to better understand these platforms, this field is still in its infancy as much work still needs to be conducted especially on the biological interface. From a chemistry perspective, researchers in the MOF field have mastered designing and synthesizing different sizes, morphologies and topologies; however, advancement on the biological front is still comparatively limited. More *in vivo* work should take place to better assess the pharmacokinetics profile of these platforms especially in terms of degradability and toxicity. It is also important to study the interaction of MOFs with different proteins in the body and to analyze the protein corona after various proteins attach to the surface, which has been well explored for other nanoparticles. Moreover, colloidal stability is a key factor in pharmaceutical formulations and needs to be very well studied if these platforms are to have a real shot at making it to the consumer market. It is very clear that there is much to be done on the forefront of MOFs for biomedical applications but this is exactly what makes this field of research

very intriguing. Researchers in this field are able to embark on a very new journey and thus have the chance to be the pioneers in unraveling the story of MOFs in the biological world.

Conflicts of interest

There are no conflicts to declare.

References

1 S. L. James, *Chem. Soc. Rev.*, 2003, **32**, 276–288.
2 K. M. Choi, K. Na, G. A. Somorjai and O. M. Yaghi, *J. Am. Chem. Soc.*, 2015, **137**, 7810–7816.
3 H. Li, M. Eddaoudi, T. L. Groy and O. M. Yaghi, *J. Am. Chem. Soc.*, 1998, **120**, 8571–8572.
4 B. Chen, C. Liang, J. Yang, D. S. Contreras, Y. L. Clancy, E. B. Lobkovsky, O. M. Yaghi and S. Dai, *Angew. Chem., Int. Ed.*, 2006, **45**, 1390–1393.
5 J. L. C. Rowsell and O. M. Yaghi, *J. Am. Chem. Soc.*, 2006, **128**, 1304–1315.
6 M. Eddaoudi, J. Kim, N. Rosi, D. Vodak, J. Wachter, M. Keeffe and O. M. Yaghi, *Science*, 2002, **295**, 469.
7 T. Devic, P. Horcajada, C. Serre, F. Salles, G. Maurin, B. Moulin, D. Heurtaux, G. Clet, A. Vimont, J.-M. Grenèche, B. L. Ouay, F. Moreau, E. Magnier, Y. Filinchuk, J. Marrot, J.-C. Lavalley, M. Daturi and G. Férey, *J. Am. Chem. Soc.*, 2010, **132**, 1127–1136.
8 Z. Wang, K. K. Tanabe and S. M. Cohen, *Inorg. Chem.*, 2009, **48**, 296–306.
9 S. S. Kaye and J. R. Long, *J. Am. Chem. Soc.*, 2008, **130**, 806–807.
10 Y. K. Hwang, D.-Y. Hong, J.-S. Chang, S. H. Jhung, Y.-K. Seo, J. Kim, A. Vimont, M. Daturi, C. Serre and G. Férey, *Angew. Chem., Int. Ed.*, 2008, **47**, 4144–4148.
11 I. Abánades Lázaro, S. Haddad, S. Sacca, C. Orellana-Tavra, D. Fairen-Jimenez and R. S. Forgan, *Chem*, 2017, **2**, 561–578.
12 S.-Z. Ren, D. Zhu, X.-H. Zhu, B. Wang, Y.-S. Yang, W.-X. Sun, X.-M. Wang, P.-C. Lv, Z.-C. Wang and H.-L. Zhu, *ACS Appl. Mater. Interfaces*, 2019, **11**, 20678–20688.
13 S. Wuttke, M. Lismont, A. Escudero, B. Rungtaweevoranit and W. J. Parak, *Biomaterials*, 2017, **123**, 172–183.
14 K. Liang, R. Ricco, C. M. Doherty, M. J. Styles, S. Bell, N. Kirby, S. Mudie, D. Haylock, A. J. Hill, C. J. Doonan and P. Falcaro, *Nat. Commun.*, 2015, **6**, 7240.
15 M. Peller, K. Böll, A. Zimpel and S. Wuttke, *Inorg. Chem. Front.*, 2018, **5**, 1760–1779.
16 J. Xiao, Y. Zhu, S. Huddleston, P. Li, B. Xiao, O. K. Farha and G. A. Ameer, *ACS Nano*, 2018, **12**, 1023–1032.
17 B. Steinborn, P. Hirschle, M. Höhn, T. Bauer, M. Barz, S. Wuttke, E. Wagner and U. Lächelt, *Adv. Ther.*, 2019, **2**, 1900120.
18 E. Ploetz, A. Zimpel, V. Cauda, D. Bauer, D. C. Lamb, C. Haisch, S. Zahler, A. M. Vollmar, S. Wuttke and H. Engelke, *Adv. Mater.*, 2020, **32**, 1907267.
19 A. Poddar, S. Pyreddy, F. Carraro, S. Dhakal, A. Rassell, M. R. Field, T. S. Reddy, P. Falcaro, C. M. Doherty and R. Shukla, *Chem. Commun.*, 2020, **56**, 15406–15409.
20 Y. Chen, P. Li, J. A. Modica, R. J. Drout and O. K. Farha, *J. Am. Chem. Soc.*, 2018, **140**, 5678–5681.
21 R. J. Drout, L. Robison and O. K. Farha, *Coord. Chem. Rev.*, 2019, **381**, 151–160.
22 S. Wang, Y. Chen, S. Wang, P. Li, C. A. Mirkin and O. K. Farha, *J. Am. Chem. Soc.*, 2019, **141**, 2215–2219.
23 J. Yang and Y.-W. Yang, *Small*, 2020, **16**, 1906846.
24 M. d. J. Velásquez-Hernández, M. Linares-Moreau, E. Astria, F. Carraro, M. Z. Alyami, N. M. Khashab, C. J. Sumby, C. J. Doonan and P. Falcaro, *Coord. Chem. Rev.*, 2021, **429**, 213651.
25 M. Giménez-Marqués, T. Hidalgo, C. Serre and P. Horcajada, *Coord. Chem. Rev.*, 2016, **307**, 342–360.
26 K. Sun, L. Li, X. Yu, L. Liu, Q. Meng, F. Wang and R. Zhang, *J. Colloid Interface Sci.*, 2017, **486**, 128–135.
27 L. Li, Y. Q. Wu, K. K. Sun, R. Zhang, L. Fan, K. K. Liang and L. B. Mao, *Mater. Lett.*, 2016, **162**, 207–210.
28 P. Horcajada, R. Gref, T. Baati, P. K. Allan, G. Maurin, P. Couvreur, G. Férey, R. E. Morris and C. Serre, *Chem. Rev.*, 2012, **112**, 1232–1268.
29 M. Hoop, C. F. Walde, R. Riccò, F. Mushtaq, A. Terzopoulou, X.-Z. Chen, A. J. deMello, C. J. Doonan, P. Falcaro, B. J. Nelson, J. Puigmartí-Luis and S. Pané, *Appl. Mater. Today*, 2018, **11**, 13–21.
30 I. Abánades Lázaro and R. S. Forgan, *Coord. Chem. Rev.*, 2019, **380**, 230–259.
31 H. Cai, Y.-L. Huang and D. Li, *Coord. Chem. Rev.*, 2019, **378**, 207–221.
32 S. Rojas, A. Arenas-Vivo and P. Horcajada, *Coord. Chem. Rev.*, 2019, **388**, 202–226.
33 S. Wuttke, A. Zimpel, T. Bein, S. Braig, K. Stoiber, A. Vollmar, D. Müller, K. Haastert-Talini, J. Schaeske, M. Stiesch, G. Zahn, A. Mohmeyer, P. Behrens, O. Eickelberg, D. A. Bölükbas and S. Meiners, *Adv. Healthcare Mater.*, 2017, **6**, 1600818.
34 W. Liang, P. Wied, F. Carraro, C. J. Sumby, B. Nidetzky, C.-K. Tsung, P. Falcaro and C. J. Doonan, *Chem. Rev.*, 2021, **121**, 1077–1129.
35 E. Borenfreund and J. A. Puerner, *Toxicology*, 1986, **39**, 121–134.
36 C. Tamames-Tabar, D. Cunha, E. Imbuluzqueta, F. Ragon, C. Serre, M. J. Blanco-Prieto and P. Horcajada, *J. Mater. Chem. B*, 2014, **2**, 262–271.
37 R. Grall, T. Hidalgo, J. Delic, A. Garcia-Marquez, S. Chevillard and P. Horcajada, *J. Mater. Chem. B*, 2015, **3**, 8279–8292.
38 M. Z. Alyami, S. K. Alsaiari, Y. Li, S. S. Qutub, F. A. Aleisa, R. Sougrat, J. S. Merzaban and N. M. Khashab, *J. Am. Chem. Soc.*, 2020, **142**, 1715–1720.
39 M. Cai, L. Qin, L. Pang, B. Ma, J. Bai, J. Liu, X. Dong, X. Yin and J. Ni, *New J. Chem.*, 2020, **44**, 17693–17704.
40 T. Baati, L. Njim, F. Neffati, A. Kerkeni, M. Bouttemi, R. Gref, M. F. Najjar, A. Zakhama, P. Couvreur, C. Serre and P. Horcajada, *Chem. Sci.*, 2013, **4**, 1597–1607.

41 M. T. Simon-Yarza, T. Baati, A. Paci, L. L. Lesueur, A. Seck, M. Chiper, R. Gref, C. Serre, P. Couvreur and P. Horcajada, *J. Mater. Chem. B*, 2016, **4**, 585–588.
42 K. Ni, T. Aung, S. Li, N. Fatuzzo, X. Liang and W. Lin, *Chem*, 2019, **5**, 1892–1913.
43 X. Zhong, Y. Zhang, L. Tan, T. Zheng, Y. Hou, X. Hong, G. Du, X. Chen, Y. Zhang and X. Sun, *J. Controlled Release*, 2019, **300**, 81–92.
44 S. K. Alsaiari, S. S. Qutub, S. Sun, W. Baslyman, M. Aldehaiman, M. Alyami, A. Almalik, R. Halwani, J. Merzaban, Z. Mao and N. M. Khashab, *Sci. Adv.*, 2021, **7**, eabe7174.
45 D. van der Merwe, S. Tawde, J. A. Pickrell and L. E. Erickson, *Cutan. Ocul. Toxicol.*, 2009, **28**, 78–82.
46 P. Horcajada, F. Salles, S. Wuttke, T. Devic, D. Heurtaux, G. Maurin, A. Vimont, M. Daturi, O. David, E. Magnier, N. Stock, Y. Filinchuk, D. Popov, C. Riekel, G. Férey and C. Serre, *J. Am. Chem. Soc.*, 2011, **133**, 17839–17847.
47 T. R. Whitfield, X. Wang, L. Liu and A. J. Jacobson, *Solid State Sci.*, 2005, **7**, 1096–1103.
48 C. Serre, C. Mellot-Draznieks, S. Surblé, N. Audebrand, Y. Filinchuk and G. Férey, *Science*, 2007, **315**, 1828.
49 S. Hou, Y.-n. Wu, L. Feng, W. Chen, Y. Wang, C. Morlay and F. Li, *Dalton Trans.*, 2018, **47**, 2222–2231.
50 M. Dan-Hardi, C. Serre, T. Frot, L. Rozes, G. Maurin, C. Sanchez and G. Férey, *J. Am. Chem. Soc.*, 2009, **131**, 10857–10859.
51 H. Li, M. Eddaoudi, M. O'Keeffe and O. M. Yaghi, *Nature*, 1999, **402**, 276–279.
52 R. Banerjee, H. Furukawa, D. Britt, C. Knobler, M. O'Keeffe and O. M. Yaghi, *J. Am. Chem. Soc.*, 2009, **131**, 3875–3877.
53 X.-C. Huang, Y.-Y. Lin, J.-P. Zhang and X.-M. Chen, *Angew. Chem., Int. Ed.*, 2006, **45**, 1557–1559.
54 J.-P. Zhang and X.-M. Chen, *Chem. Commun.*, 2006, 1689–1699, DOI: 10.1039/B516367F.
55 Y. Liu, V. C. Kravtsov, R. Larsen and M. Eddaoudi, *Chem. Commun.*, 2006, 1488–1490, DOI: 10.1039/B600188M.
56 I. Imaz, M. Rubio-Martínez, J. An, I. Solé-Font, N. L. Rosi and D. Maspoch, *Chem. Commun.*, 2011, **47**, 7287–7302.
57 S.-P. Wu and C.-H. Lee, *CrystEngComm*, 2009, **11**, 219–222.
58 J. An, S. J. Geib and N. L. Rosi, *J. Am. Chem. Soc.*, 2009, **131**, 8376–8377.
59 C. Serre, F. Millange, S. Surblé and G. Férey, *Angew. Chem., Int. Ed.*, 2004, **43**, 6285–6289.
60 C. Serre, S. Surblé, C. Mellot-Draznieks, Y. Filinchuk and G. Férey, *Dalton Trans.*, 2008, 5462–5464, DOI: 10.1039/B805408H.
61 Y. Furukawa, T. Ishiwata, K. Sugikawa, K. Kokado and K. Sada, *Angew. Chem., Int. Ed.*, 2012, **51**, 10566–10569.
62 S. Krishnan, V. Mani, D. Wasalathanthri, C. V. Kumar and J. F. Rusling, *Angew. Chem., Int. Ed.*, 2011, **50**, 1175–1178.
63 J. Park, Q. Jiang, D. Feng, L. Mao and H.-C. Zhou, *J. Am. Chem. Soc.*, 2016, **138**, 3518–3525.
64 A. Baeza, D. Ruiz-Molina and M. Vallet-Regí, *Expert Opin. Drug Delivery*, 2017, **14**, 783–796.
65 D. Duan, H. Liu, M. Xu, M. Chen, Y. Han, Y. Shi and Z. Liu, *ACS Appl. Mater. Interfaces*, 2018, **10**, 42165–42174.
66 Z. Zhu, S. Jiang, Y. Liu, X. Gao, S. Hu, X. Zhang, C. Huang, Q. Wan, J. Wang and X. Pei, *Nano Res.*, 2020, **13**, 511–526.
67 M.-H. Pham, G.-T. Vuong, A.-T. Vu and T.-O. Do, *Langmuir*, 2011, **27**, 15261–15267.
68 P. Horcajada, C. Serre, D. Grosso, C. Boissière, S. Perruchas, C. Sanchez and G. Férey, *Adv. Mater.*, 2009, **21**, 1931–1935.
69 W. J. Rieter, K. M. L. Taylor, H. An, W. Lin and W. Lin, *J. Am. Chem. Soc.*, 2006, **128**, 9024–9025.
70 L.-G. Qiu, Z.-Q. Li, Y. Wu, W. Wang, T. Xu and X. Jiang, *Chem. Commun.*, 2008, 3642–3644, DOI: 10.1039/B804126A.
71 K. M. L. Taylor, W. J. Rieter and W. Lin, *J. Am. Chem. Soc.*, 2008, **130**, 14358–14359.
72 W. Yang, J. Feng and H. Zhang, *J. Mater. Chem.*, 2012, **22**, 6819–6823.
73 S. Wang, Y. Lv, Y. Yao, H. Yu and G. Lu, *Inorg. Chem. Commun.*, 2018, **93**, 56–60.
74 N. Feliu and B. Fadeel, *Nanoscale*, 2010, **2**, 2514–2520.
75 J. A. Champion, Y. K. Katare and S. Mitragotri, *J. Controlled Release*, 2007, **121**, 3–9.
76 N. u. Qadir, S. A. M. Said and H. M. Bahaidarah, *Microporous Mesoporous Mater.*, 2015, **201**, 61–90.
77 H. Jasuja and K. S. Walton, *Dalton Trans.*, 2013, **42**, 15421–15426.
78 L. Huang, H. Wang, J. Chen, Z. Wang, J. Sun, D. Zhao and Y. Yan, *Microporous Mesoporous Mater.*, 2003, **58**, 105–114.
79 J. A. Greathouse and M. D. Allendorf, *J. Am. Chem. Soc.*, 2006, **128**, 10678–10679.
80 J. Liu, F. Zhang, X. Zou, G. Yu, N. Zhao, S. Fan and G. Zhu, *Chem. Commun.*, 2013, **49**, 7430–7432.
81 N. J. Hinks, A. C. McKinlay, B. Xiao, P. S. Wheatley and R. E. Morris, *Microporous Mesoporous Mater.*, 2010, **129**, 330–334.
82 D. Feng, Z.-Y. Gu, J.-R. Li, H.-L. Jiang, Z. Wei and H.-C. Zhou, *Angew. Chem., Int. Ed.*, 2012, **51**, 10307–10310.
83 M. A. Luzuriaga, C. E. Benjamin, M. W. Gaertner, H. Lee, F. C. Herbert, S. Mallick and J. J. Gassensmith, *Supramol. Chem.*, 2019, **31**, 485–490.
84 P. Küsgens, M. Rose, I. Senkovska, H. Fröde, A. Henschel, S. Siegle and S. Kaskel, *Microporous Mesoporous Mater.*, 2009, **120**, 325–330.
85 J. B. DeCoste, G. W. Peterson, H. Jasuja, T. G. Glover, Y.-G. Huang and K. S. Walton, *J. Mater. Chem. A*, 2013, **1**, 5642–5650.
86 Y. L. Liu, X. J. Zhao, X. X. Yang and Y. F. Li, *Analyst*, 2013, **138**, 4526–4531.
87 A. Bartolazzi, R. Peach, A. Aruffo and I. Stamenkovic, *J. Exp. Med.*, 1994, **180**, 53–66.
88 Y. Yang, Y.-R. Yao, Y.-J. Jin and X. Jia, *Chem. – Eur. J.*, 2020, **27**, 2987–2992.
89 S. Wuttke, S. Braig, T. Preiß, A. Zimpel, J. Sicklinger, C. Bellomo, J. O. Rädler, A. M. Vollmar and T. Bein, *Chem. Commun.*, 2015, **51**, 15752–15755.

90 B. Illes, P. Hirschle, S. Barnert, V. Cauda, S. Wuttke and H. Engelke, *Chem. Mater.*, 2017, **29**, 8042–8046.
91 Z. Luo, L. Jiang, S. Yang, Z. Li, W. M. W. Soh, L. Zheng, X. J. Loh and Y.-L. Wu, *Adv. Healthcare Mater.*, 2019, **8**, 1900406.
92 S. K. Alsaiari, S. Patil, M. Alyami, K. O. Alamoudi, F. A. Aleisa, J. S. Merzaban, M. Li and N. M. Khashab, *J. Am. Chem. Soc.*, 2018, **140**, 143–146.
93 C. Orellana-Tavra, M. Köppen, A. Li, N. Stock and D. Fairen-Jimenez, *ACS Appl. Mater. Interfaces*, 2020, **12**, 5633–5641.
94 R. Xie, P. Yang, S. Peng, Y. Cao, X. Yao, S. Guo and W. Yang, *J. Mater. Chem. B*, 2020, **8**, 6128–6138.
95 K. Zhang, X. Meng, Z. Yang, H. Dong and X. Zhang, *Biomaterials*, 2020, **258**, 120278.
96 J. Zhuang, Y. Duan, Q. Zhang, W. Gao, S. Li, R. H. Fang and L. Zhang, *Nano Lett.*, 2020, **20**, 4051–4058.
97 Y. Xiao, W. Huang, D. Zhu, Q. Wang, B. Chen, Z. Liu, Y. Wang and Q. Liu, *RSC Adv.*, 2020, **10**, 7194–7205.
98 Y. Lin, Y. Zhong, Y. Chen, L. Li, G. Chen, J. Zhang, P. Li, C. Zhou, Y. Sun, Y. Ma, Z. Xie and Q. Liao, *Mol. Pharmaceutics*, 2020, **17**, 3328–3341.
99 H. Maeda, J. Wu, T. Sawa, Y. Matsumura and K. Hori, *J. Controlled Release*, 2000, **65**, 271–284.
100 P. Horcajada, T. Chalati, C. Serre, B. Gillet, C. Sebrie, T. Baati, J. F. Eubank, D. Heurtaux, P. Clayette, C. Kreuz, J.-S. Chang, Y. K. Hwang, V. Marsaud, P.-N. Bories, L. Cynober, S. Gil, G. Férey, P. Couvreur and R. Gref, *Nat. Mater.*, 2010, **9**, 172–178.
101 W.-L. Liu, M.-Z. Zou, S.-Y. Qin, Y.-J. Cheng, Y.-H. Ma, Y.-X. Sun and X.-Z. Zhang, *Adv. Funct. Mater.*, 2020, **30**, 2003559.
102 H. Min, J. Wang, Y. Qi, Y. Zhang, X. Han, Y. Xu, J. Xu, Y. Li, L. Chen, K. Cheng, G. Liu, N. Yang, Y. Li and G. Nie, *Adv. Mater.*, 2019, **31**, 1808200.
103 Y.-B. Miao, W.-Y. Pan, K.-H. Chen, H.-J. Wei, F.-L. Mi, M.-Y. Lu, Y. Chang and H.-W. Sung, *Adv. Funct. Mater.*, 2019, **29**, 1904828.
104 K. Ni, T. Luo, G. T. Nash and W. Lin, *Acc. Chem. Res.*, 2020, **53**, 1739–1748.
105 F. Jeremias, S. K. Henninger and C. Janiak, *Dalton Trans.*, 2016, **45**, 8637–8644.
106 M. Ma, A. Bétard, I. Weber, N. S. Al-Hokbany, R. A. Fischer and N. Metzler-Nolte, *Cryst. Growth Des.*, 2013, **13**, 2286–2291.
107 S. Jafari, F. Ghorbani-Shahna, A. Bahrami and H. Kazemian, *Appl. Sci.*, 2018, **8**, 310.
108 L. Feng, Y. Wang, S. Yuan, K.-Y. Wang, J.-L. Li, G. S. Day, D. Qiu, L. Cheng, W.-M. Chen, S. T. Madrahimov and H.-C. Zhou, *ACS Catal.*, 2019, **9**, 5111–5118.
109 P. Niu, N. Lu, J. Liu, H. Jia, F. Zhou, B. Fan and R. Li, *Microporous Mesoporous Mater.*, 2019, **281**, 92–100.
110 H. Reinsch, *Eur. J. Inorg. Chem.*, 2016, 4290–4299.
111 M. d. J. Velásquez-Hernández, R. Ricco, F. Carraro, F. T. Limpoco, M. Linares-Moreau, E. Leitner, H. Wiltsche, J. Rattenberger, H. Schröttner, P. Frühwirt, E. M. Stadler, G. Gescheidt, H. Amenitsch, C. J. Doonan and P. Falcaro, *CrystEngComm*, 2019, **21**, 4538–4544.
112 C. Tamames-Tabar, D. Cunha, E. Imbuluzqueta, F. Ragon, C. Serre, M. J. Blanco-Prieto and P. Horcajada, *J. Mater. Chem. B*, 2014, **2**, 262–271.
113 P. Kush, T. Bajaj, M. Kaur, J. Madan, U. K. Jain, P. Kumar, A. Deep and K.-H. Kim, *J. Inorg. Organomet. Polym. Mater.*, 2020, **30**, 2827–2841.
114 M. T. Simon-Yarza, T. Baati, A. Paci, L. L. Lesueur, A. Seck, M. Chiper, R. Gref, C. Serre, P. Couvreur and P. Horcajada, *J. Mater. Chem. B*, 2016, **4**, 585–588.
115 M. Ma, H. Noei, B. Mienert, J. Niesel, E. Bill, M. Muhler, R. A. Fischer, Y. Wang, U. Schatzschneider and N. Metzler-Nolte, *Chem. – Eur. J.*, 2013, **19**, 6785–6790.
116 T. Baati, L. Njim, F. Neffati, A. Kerkeni, M. Bouttemi, R. Gref, M. F. Najjar, A. Zakhama, P. Couvreur, C. Serre and P. Horcajada, *Chem. Sci.*, 2013, **4**, 1597–1607.
117 S. Zuluaga, E. M. A. Fuentes-Fernandez, K. Tan, F. Xu, J. Li, Y. J. Chabal and T. Thonhauser, *J. Mater. Chem. A*, 2016, **4**, 5176–5183.
118 J. Hu, Y. Chen, H. Zhang and Z. Chen, *J. Solid State Chem.*, 2021, **294**, 121853.
119 Q. Cheng, W. Yu, J. Ye, M. Liu, W. Liu, C. Zhang, C. Zhang, J. Feng and X.-Z. Zhang, *Biomaterials*, 2019, **224**, 119500.
120 X. Leng, H. Huang, W. Wang, N. Sai, L. You, X. Yin and J. Ni, *J. Evidence-Based Complementary Altern. Med.*, 2018, **2018**, 3249023.
121 D. Cunha, M. Ben Yahia, S. Hall, S. R. Miller, H. Chevreau, E. Elkaïm, G. Maurin, P. Horcajada and C. Serre, *Chem. Mater.*, 2013, **25**, 2767–2776.
122 Y. Wang, W. Lin, S. Yu, X. Huang, X. Lang, Q. He, L. Gao, H. Zhu and J. Chen, *J. Solid State Chem.*, 2021, **293**, 121805.
123 D. Chen, D. Yang, C. A. Dougherty, W. Lu, H. Wu, X. He, T. Cai, M. E. Van Dort, B. D. Ross and H. Hong, *ACS Nano*, 2017, **11**, 4315–4327.